Hue University Journal of Science: Natural Science; ISSN 1859–1388

Vol. 127, No. 1D, 2018, P. 5–12; DOI: 10.26459/hueuni-jns.v127i1A.5007

FACILE SYNTHESIS OF HIGH POROUS NiO NANOSTRUCTURES BY HYDROTHERMAL METHOD

Pham Long Quang[1], Nguyen Thi Ngoc Anh[3], Tran Xuan Mau[1], Nguyen Duc Cuong[1,2]*

[1] University of Sciences, Hue University, 77 Nguyen Hue St., Hue, Vietnam
[2] School of Hospitality and Tourism, Hue University, 22 Lam Hoang St., Hue, Viet Nam
[3] University of Education, Hue University, 34 Le Loi St., Hue, Vietnam

Abstract. In this report, a simple hydrothermal approach to the fabrication of porous NiO nanospheres and nanotoroids was described. The morphologies and crystal structure of the as-fabricated nanomaterials were characterized using SEM, TEM, XRD, EDS, and N_2 adsorption/desorption isotherm. The results showed that the porous NiO nanospheres have the diameter ranging from 2 to 10 μm, and they are self-assembled nanoparticles (NPs). The nanotoroids have an average outer diameter and inner diameter of ~300 nm and ~60 nm, respectively. This simple and mild approach to fabricate highly porous NiO nanostructures could be easily scaled up and potentially extended to the synthesis of other porous nanostructured metal oxides.

Keywords: NiO, porous nanomaterial, nanosphere, nanotoroid

1 Introduction

Up to now, metal oxide nanostructures with intriguing geometries have been widely investigated to explore their novel physicochemical features such as electrical, magnetic, optical, and catalytic properties [1]. These new properties of metal oxide nanostructures could originate from the intrinsic properties of the metal oxide with its metal without completely filled d-shells [2] as well as the limited size and high density of their corner/edge surface sites associated with the shape effect [3]. Thus, metal oxide nanostructures are considered as the most attractive functional materials and have also opened up a new avenue for various technological applications [4].

Nickel oxide (NiO), which is an important p-type semiconductor, has been extensively investigated for many areas of applications [5]. Their low cost, wide band gap, unique electronic properties, chemical and thermal stability, and environmentally friendly nature are appealing features for researchers [6]. Various morphologies of NiO have been successfully synthesized such as nanowires [7], nano-flowers [8], and nano-sheets [9]. Significant works have indicated that the nano-materials based on high porous NiO architectures often have novel

* *Corresponding: nguyenduccuong@hueuni.edu.vn*

Submitted: 4–10–2018; Revised: 02–11–2018; Accepted: 6–1–2018

physicochemical properties [10]. Yuan et al. [10] reported that hierarchical porous NiO nano-spherical superstructures have a large specific energy density, high rate capability, and good electrochemical stability, which was expected as a low-cost, potential super-capacitor material. The mesoporous Cu-doped NiO nanostructures, which were used as anode lithium-ion battery materials, exhibited greatly enhanced electrochemical performance with high reversible and high rate capacity [11]. Yu et al. [12] presented that the uniform porous NiO nano-sheets showed as an effective, active and stable catalyst for methane deep oxidation because they have a high specific surface area, large pore size and pore volume. Therefore, the development of facile synthesis and thorough understanding of the formation mechanism for the high porous NiO nanostructures have great importance.

Herein, we synthesize high porous NiO with hierarchical porous nanospheres and nanotoroids by simple hydrothermal methods. $Ni(NO_3)_2$, NaOH and $(NH_2)_2CO$) were used as starting materials to form NiO nanospheres and nanotoroids. The obtained NiO nanostructures have a high specific surface area and porosity and contain many mesopores.

2 Experimental

2.1 Synthesis of NiO nanotoroids

Porous NiO nanotoroids were fabricated by means of a simple hydrothermal approach using $Ni(NO_3)_2{\cdot}6H_2O$ (Sigma-Aldrich, Germany, p. a., ≥98.5% (KT)) and NaOH (Sigma-Aldrich, Germany) as starting materials. In a typical procedure, 11.64 g of $Ni(NO_3)_2$ and 2 g of NaOH were dissolved in 40 mL distilled water under magnetic stirring for 10 min at room temperature. After that, the obtained suspension was transferred into a Teflon-lined stainless steel autoclave (50 mL) and then annealed at 185 °C for 8 h. The powder was collected by centrifugation and washed with distilled water and ethanol several times. The production was dried at 60 °C for 24 h and then calcined at 600 °C for 5 h to form NiO nanotoroids.

2.2 Synthesis of porous NiO nanospheres

The porous NiO nanospheres were also synthesized by means of a facile hydrothermal method using $Ni(NO_3)_2{\cdot}6H_2O$ (Sigma-Aldrich, Germany, p. a., ≥98.5% (KT)) and $(NH_2)_2CO$ (Sigma-Aldrich, Germany) as starting materials. Typically, 1.24 g of $Ni(NO_3)_2$ and 13.5 g of urea were dissolved in 435 mL distilled water under magnetic stirring for 15 min at room temperature. The solution was then transferred into a Teflon-lined stainless steel autoclave (500 mL) and heated at 60 °C for 12 h. After that, the hydrothermal temperature was increased to 90 °C and kept at this temperature for 8 h. The powder was collected by centrifugation and washed with ethanol and distilled water several times. The precipitation was annealed at 600 °C for 5 h to form NiO porous nanospheres.

2.3 Material characterization

The as-synthesized NiO nanostructures were characterized using scanning electron microscopy (SEM, JSM-5300LV), energy dispersive X-ray spectroscopy (EDS), transmission electron microscopy (TEM, JEOL, JEM 1230), X-ray diffraction (XRD, D8 Advance, Brucker), and nitrogen adsorption/desorption isotherms (Autosorb-iQ) to clearly demonstrate their microstructures and morphologies.

3 Results and discussion

The SEM and TEM images of the as-fabricated porous NiO nanostructure are shown in Fig. 1. As can be seen in low magnification SEM images, the obtained sample is spherical in morphology (Fig. 1 (a) and (b)). The micro-particles are highly dispersed with a rough surface and their sphere diameter ranging from 2 to 10 μm. The high magnification SEM image shows that the spherical particles were formed from NiO nanoparticle agglomerates (Fig. 1 (c)). The TEM image of NiO microspheres shows clearly dark skeletons and bright pores, which confirms the formation of porous NiO microspheres [13] and is in a good agreement with SEM results.

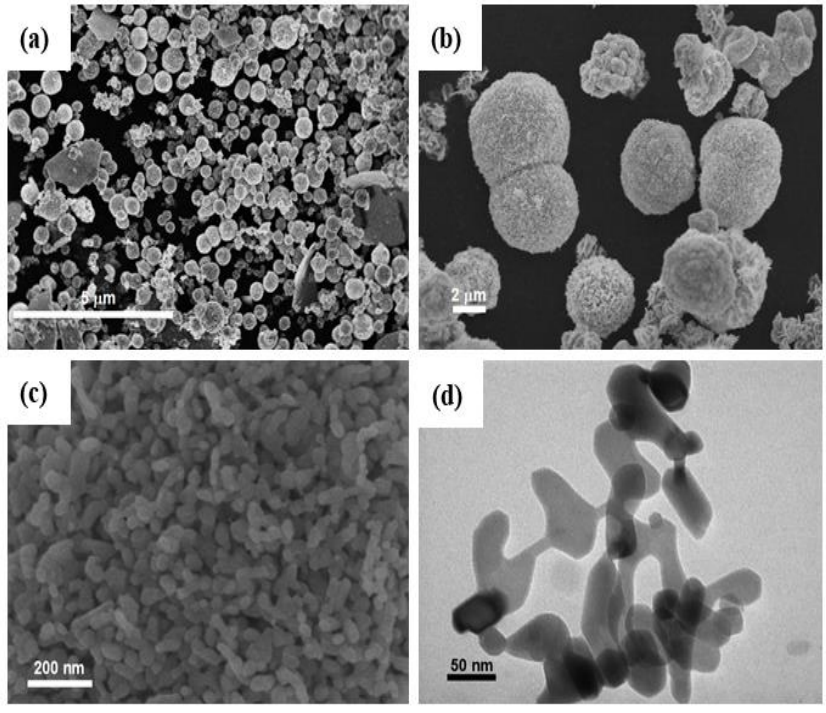

Fig. 1. SEM images (a–c) and TEM image (d) of the porous NiO nanospheres.

The morphologies of NiO nanotoroids are shown in Fig. 2. As can be seen in SEM images, the obtained materials present toroid-shaped nanostructures with a uniform morphology (Fig. 2 (a) and (b)). The TEM images clearly exhibit that the monodisperse nanotoroid contains an interior hollow place with its average outer particle diameter and inner diameter of ~300 nm and ~60 nm, respectively (Fig. 2 (c) and (d)).

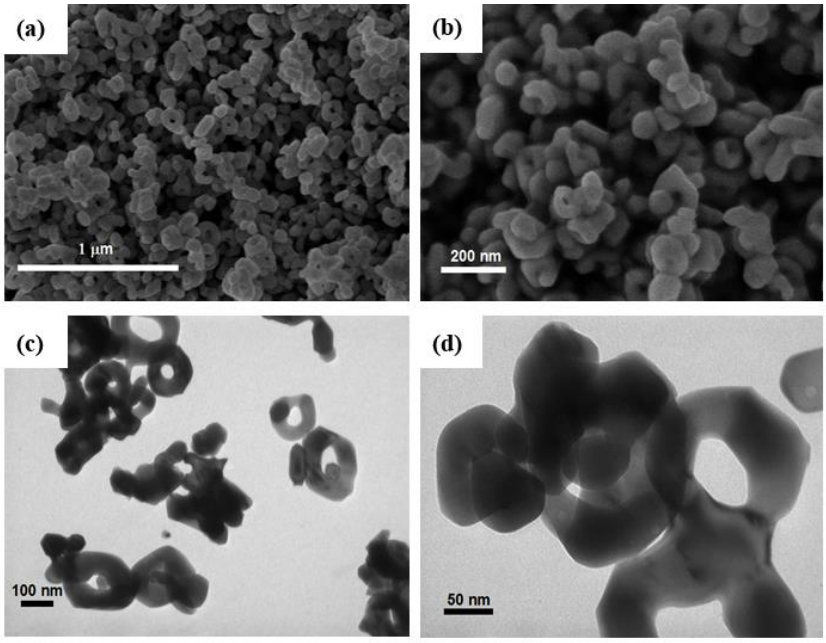

Fig. 2. SEM (a, b) and TEM (c, d) images of nanotoroids.

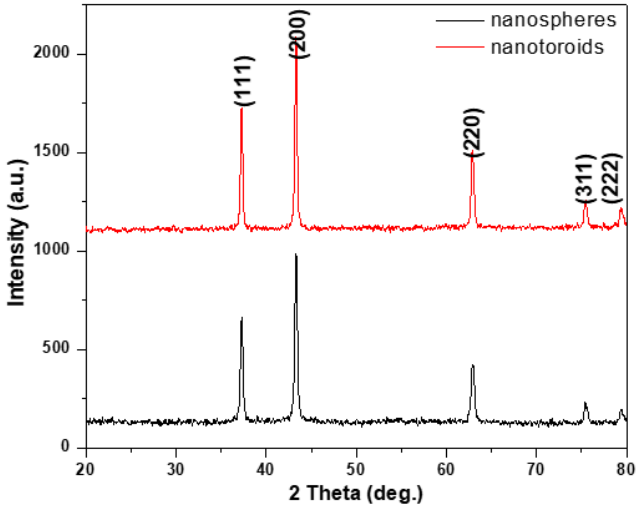

Fig. 3. XRD pattern of NiO nanotoroids and NiO nanospheres.

The XRD patterns of the formed NiO nanospheres and nanotoroids are shown in Fig. 3. The diffraction peaks at the 2θ angle of about 37.3°, 43.3°, 62.9°, 75.3° and 79.4° could be indexed as (111), (200), (220), (311), and (222) lattice planes according to JCPDS No. 47-1049. The high-intensity and sharp diffraction peaks imply that the porous nanostructures have high crystallinity. No peaks from other phases are found, indicating the synthesized samples have high purity.

The chemical composition of NiO nanospheres and NiO nanotoroids was also analyzed using the energy dispersive X-ray spectrum (EDS) technique. The typical EDS spectra of the two samples show the presence of Ni and O (Fig. 4). The mass composition of Ni and O for the nanospheres and the nanotoroids were 79.09, 20.91% and 79.17, 20.83%, respectively (Table 1). For both samples, the calculated atomic ratio of Ni/O is about 1/1, indicating that the chemical formula of the as-fabricated nanostructures is NiO. The results are in a good agreement with the XRD pattern observations.

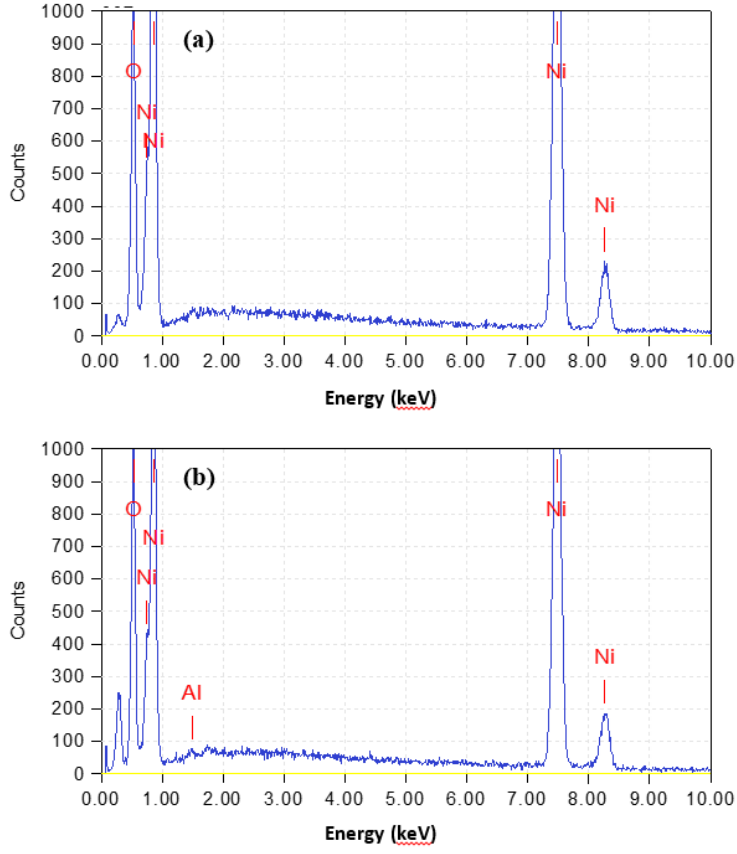

Fig. 4. EDS of NiO nanotoroids (a) and NiO nanospheres (b).

Table 1. Major elemental components of NiO nanotoroids and NiO nanospheres analyzed using EDX

Sample	Element	Mass (%)	Atom (%)	Error (%)
NiO nanotoroids	**Ni K**	79.17	50.89	0.27
	O K	20.83	49.11	0.07
NiO nanospheres	**Ni K**	79.09	50.76	0.31
	O K	20.91	49.24	0.08

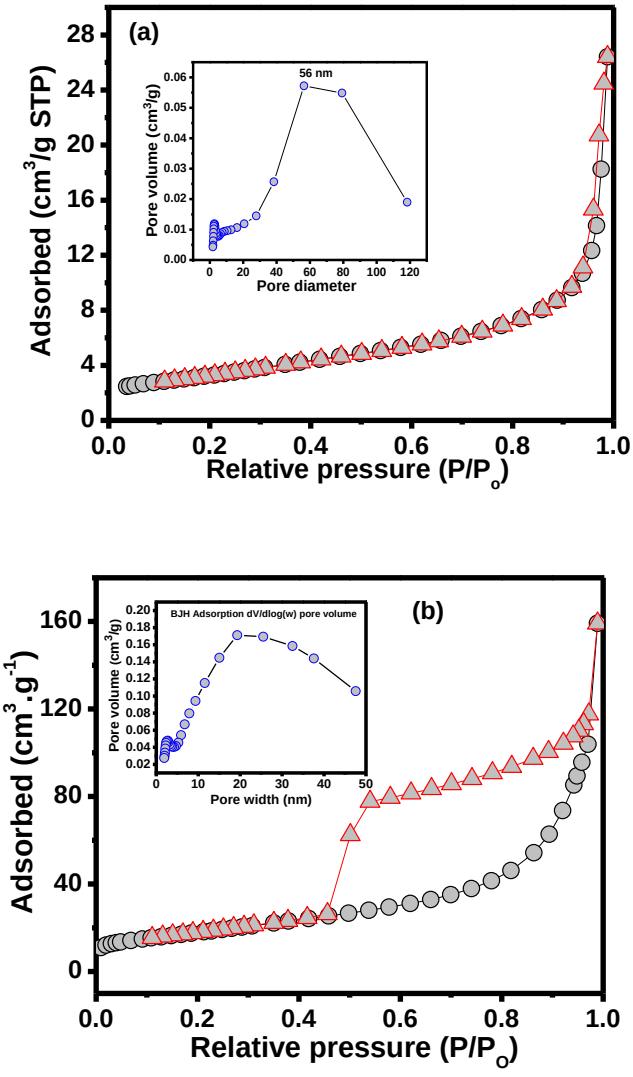

Fig. 5. N_2 adsorption/desorption isotherms and pore diameter distribution of (a) NiO nanotoroids and (b) nanospheres.

The porosities of the NiO nanostructures were distinctly characterized using N_2 adsorption/desorption isotherm. Fig. 5 (a) shows that the NiO nanotoroids exhibit the adsorption/desorption isotherm of the shape of the IV type hysteresis loop according to the IUPAC classification with the H1 hysteresis loop that indicates mesoporous structures [14]. The BJH pore size distribution of the nanotoroids (inset of Fig. 5 (a)) assigns the bimodal pore size distribution in the mesoporous and macroporous region. The specific surface area obtained using the BET method for this sample is 18 m^2/g. The adsorption/desorption N_2 isotherm of the nanospheres shown in Fig. 5 (b) indicates that the nanomaterials have the type IV isotherm with the H3 hysteresis loop with a mesoporous structure [15]. The BET surface area and BJH pore size distributions (inset of Fig. 5 (b)) of the nanospheres are of 64 m^2/g and 20 nm, respectively.

4 Conclusions

We have introduced two facile hydrothermal methods to fabricate highly porous NiO nanostructure using inorganic nickel salt, NaOH, and urea as starting materials. The porous NiO nanospheres with high specific surface areas were composed of many nanoparticles formed through a self-assembly process and aggregation induced during calcination. The uniform toroidal nanostructures show specific morphology with the inner diameter of ~ 60 nm and the outer diameter of ~ 300 nm. The specific architecture and porosity of the NiO nanostructures could make them an interesting system for future studies in many fields of advanced nanotechnology, particularly in catalysis, gas sensors, optics, and electronics.

Acknowledgements: The authors would like to thank the Vietnam National Foundation for Science and Technology Development (NAFOSTED) under Grant No. 103.02-2016.41 for financial support of this research.

References

1. R.S. Devan, R.A. Patil, J.H. Lin, Y.R. Ma, (2012), One-dimensional metal-oxide nanostructures: Recent developments in synthesis, characterization, and applications, *Adv. Funct. Mater.* 22, 3326–3370.
2. T. Guo, M.-S. Yao, Y.-H. Lin, C.-W. Nan, (2015), A comprehensive review on synthesis methods for transition-metal oxide nanostructures, *CrystEngComm.* 17, 3551–3585.
3. T.D. Nguyen, (2013) From formation mechanisms to synthetic methods toward shape-controlled oxide nanoparticles, *Nanoscale.* 5, 9455–9482.
4. P.L. Quang, N.D. Cuong, T.T. Hoa, H.T. Long, C.M. Hung, D.T.T. Le, N. Van Hieu, (2018), Simple post-synthesis of mesoporous p-type Co_3O_4 nanochains for enhanced H_2S gas sensing performance, Sensors Actuators, *B Chem.* 270, 158–166.

5. H. Gao, D. Wei, P. Lin, C. Liu, P. Sun, K. Shimanoe, N. Yamazoe, G. Lu, (2017), The design of excellent xylene gas sensor using Sn-doped NiO hierarchical nanostructure, Sensors Actuators, *B Chem.* 253, 1152–1162.
6. C. Feng, X. Kou, B. Chen, G. Qian, Y. Sun, G. Lu, (2017), One-pot synthesis of In doped NiO nanofibers and their gas sensing properties, Sensors Actuators, *B Chem.* 253, 584–591.
7. J. Wang, L. Wei, L. Zhang, C. Jiang, E. Siu-Wai Kong, Y. Zhang, (2012) Preparation of high aspect ratio nickel oxide nanowires and their gas sensing devices with fast response and high sensitivity, *J. Mater. Chem.* 22, 8327–8335.
8. Y. Lu, Y. Ma, S. Ma, S. Yan, (2017) Hierarchical heterostructure of porous NiO nanosheets on flower-like ZnO assembled by hexagonal nanorods for high-performance gas sensor, *Ceram. Int.* 43, 7508–7515.
9. T. Alammar, O. Shekhah, J. Wohlgemuth, A.-V. Mudring, (2012), Ultrasound-assisted synthesis of mesoporous β-$Ni(OH)_2$ and NiO nano-sheets using ionic liquids, *J. Mater. Chem.* 22, 18252–18260. doi:10.1039/c2jm32849f.
10. C. Yuan, X. Zhang, L. Su, B. Gao, L. Shen, (2009), Facile synthesis and self-assembly of hierarchical porous NiO nano/micro spherical superstructures for high performance supercapacitors, *J. Mater. Chem.* 19, 5772–5777.
11. J. Ma, L. Yin, T. Ge, (2015) 3D hierarchically mesoporous Cu-doped NiO nanostructures as high-performance anode materials for lithium ion batteries, *CrystEngComm.* 17, 9336–9347.
12. F. Yu, X. Xu, H. Peng, H. Yu, Y. Dai, W. Liu, J. Ying, Q. Sun, X. Wang, (2015), General porous NiO nano-sheet as an active and stable catalyst for CH_4 deep oxidation, *Applied Catal. A, Gen.* 507, 109–118.
13. L.H. Trinh, D.Q. Khieu, H. Thai Long, T. Thai Hoa, D. Tuan Quang, N. Duc Cuong, (2017) A novel approach for synthesis of hierarchical mesoporous Nd_2O_3 nanomaterials, *J. Rare Earths.* 35, 677–682.
14. T.D. Nguyen, C.T. Dinh, T.O. Do, (2011), Two-phase synthesis of colloidal annular-shaped $Ce_xLa_{1-x}CO_3OH$ nanoarchitectures assemblied from small particles and their thermal conversion to derived mixed oxides, *Inorg. Chem.* 50 1309–1320.
15. P. Sun, W. Wang, Y. Liu, Y. Sun, J. Ma, G. Lu, (2012), Hydrothermal synthesis of 3D urchin-like α-Fe_2O_3 nanostructure for gas sensor, *Sensors Actuators, B Chem.* 173, 52–57.